15 Accuracy Estimation and Post-Processing in Invariant Manifolds Construction

The *post-processing* algorithms are developed for the accuracy control and enhancement of approximate invariant manifold.

15.1 Formulas for Dynamic and Static Post-Processing

Assume that for the dynamical system (3.1)

$$\frac{\mathrm{d}x}{\mathrm{d}t} = J(x)$$

an approximate invariant manifold is constructed and the slow motion equations are derived:

$$\frac{\mathrm{d}x_{\mathrm{sl}}}{\mathrm{d}t} = P_{x_{\mathrm{sl}}}(J(x_{\mathrm{sl}})), x_{\mathrm{sl}} \in \Omega_{\mathrm{sl}} . \tag{15.1}$$

Here, $P_{x_{\mathrm{sl}}}$ is the projector onto the tangent space $T_{x_{\mathrm{sl}}}$ of Ω_{sl} parallel to the plain of fast motions. Suppose that we have solved the system (15.1) and have obtained $x_{\mathrm{sl}}(t)$. Let us consider the following two questions:

– How well this solution approximates the true solution $x(t)$ with the same initial condition?
– Is it possible to use the solution $x_{\mathrm{sl}}(t)$ for its refinement?

It should be stressed that these questions can be asked only if the slow system (15.1) is obtained as a result of reduction, that is, with the help of the projector $P_{x_{\mathrm{sl}}}$ that identifies fast fibers (ker $P_{x_{\mathrm{sl}}}$). These question are meaningless if "some" closure approximation is used without a specification what means "fast" and "slow" in this approximation. In the latter case one can only hope that the closure is a good guess, that it is thermodynamically consistent, etc, but nothing can be done on its refinement.

These two questions are interconnected. The first question states the problem of the *accuracy estimation*. The second states the problem of *post-processing* [348–351].

The simplest ("naive") estimation is given by the "invariance defect":

$$\Delta_{x_{\mathrm{sl}}} = (1 - P_{x_{\mathrm{sl}}})J(x_{\mathrm{sl}}) , \tag{15.2}$$

which can be compared with $J(x_{\mathrm{sl}})$. For example, this estimate is given by $\epsilon = \|\Delta_{x_{\mathrm{sl}}}\|/\|J(x_{\mathrm{sl}})\|$ using some appropriate norm.

Probably, the most comprehensive answer to the above questions can be given by solving the following equation:

$$\frac{\mathrm{d}(\delta x)}{\mathrm{d}t} = \Delta_{x_{\mathrm{sl}}(t)} + D_x J(x)|_{x_{\mathrm{sl}}(t)}\delta x \ . \tag{15.3}$$

This linear equation describes the dynamics of the variation $\delta x(t) = x(t) - x_{\mathrm{sl}}(t)$ in the linear approximation. The solution with zero initial condition $\delta x(0) = 0$ allows to estimate the robustness of x_{sl}, as well as the error. Using $x_{\mathrm{sl}}(t) + \delta x(t)$ instead of $x_{\mathrm{sl}}(t)$ gives the required solution refinement. This *dynamical post-processing* [350] allows to refine the solution substantially. However, the price for this is solving equation (15.3) with variable coefficients. The dynamical post-processing can be addressed by a whole hierarchy of simplifications, both dynamic and static. Let us mention some of them, starting from the dynamic ones.

(1) **Freezing coefficients**. In the equation (15.3) the linear operator $D_x J(x)|_{x_{\mathrm{sl}}(t)}$ is replaced by its value in some distinguished point x^* (for example, in the equilibrium) or it is frozen somehow else. As a result, one gets the equation with constant coefficients and the explicit integration formula:

$$\delta x(t) = \int_0^t exp(D^*(t - \tau))\Delta_{x_{\mathrm{sl}}(\tau)} \, \mathrm{d}\tau \ , \tag{15.4}$$

where D^* is the "frozen" operator and $\delta x(0) = 0$.

Another important way of freezing is to replace (15.3) by some *model equation*, i.e. substituting $-\frac{1}{\tau^*}$ instead of $D_x J(x)$, where τ^* is the relaxation time. In this case the formula for $\delta x(t)$ has a very simple form:

$$\delta x(t) = \int_0^t e^{\frac{\tau - t}{\tau^*}} \Delta_{x_{\mathrm{sl}}(\tau)} \, \mathrm{d}\tau \ . \tag{15.5}$$

(2) **One-dimensional Galerkin-type approximation.** Another "scalar" approximation is given by projecting (15.3) on $\Delta(t) = \Delta_{x_{\mathrm{sl}}(t)}$. Using the ansatz

$$\delta x(t) = \delta(t)\Delta(t) \ , \tag{15.6}$$

substituting it into (15.3), and projecting the result orthogonally on $\Delta(t)$ we obtain

$$\frac{\mathrm{d}\delta}{\mathrm{d}t} = 1 + \delta\frac{\langle\Delta|D\Delta\rangle - \langle\Delta|\dot{\Delta}\rangle}{\langle\Delta|\Delta\rangle} \ , \tag{15.7}$$

where $\langle|\rangle$ is an appropriate scalar product, which can depend on the point x_{sl} (for example, the entropic scalar product), $D = D_x J(x)|_{x_{\mathrm{sl}}(t)}$ or the self-adjoint linearizarion of this operator, or some approximation of it, and $\dot{\Delta} = \mathrm{d}\Delta(t)/\mathrm{d}t$.

A "hybrid" between equations (15.7) and (15.3) has a rather simple form (but it is more difficult for computations than (15.7)):

$$\frac{\mathrm{d}(\delta x)}{\mathrm{d}t} = \Delta(t) + \frac{\langle \Delta | D\Delta \rangle}{\langle \Delta | \Delta \rangle} \delta x \ . \tag{15.8}$$

Here one uses the normalized matrix element $\frac{\langle \Delta | D\Delta \rangle}{\langle \Delta | \Delta \rangle}$ instead of the linear operator $D = D_x J(x)|_{x_{\mathrm{sl}}(t)}$.

Both equations (15.7) and (15.8) can be solved explicitly:

$$\delta(t) = \int_0^t \mathrm{d}\tau \ \exp\left(\int_\tau^t k(\theta) \,\mathrm{d}\theta \right) \ , \tag{15.9}$$

$$\delta x(t) = \int_0^t \Delta(\tau) d\tau \exp\left(\int_\tau^t k_1(\theta) \,\mathrm{d}\theta \right) \ , \tag{15.10}$$

where $k(t) = \frac{\langle \Delta | D\Delta \rangle - \langle \Delta | \dot{\Delta} \rangle}{\langle \Delta | \Delta \rangle}$, $k_1(t) = \frac{\langle \Delta | D\Delta \rangle}{\langle \Delta | \Delta \rangle}$.

The projection of $\Delta_{x_{\mathrm{sl}}}(t)$ on the slow motion is equal to zero, hence, for the post-processing of the slow motion, the one-dimensional model (15.7) should be supplemented by one more iteration in order to find the first non-vanishing term in $\delta x_{\mathrm{sl}}(t)$:

$$\frac{\mathrm{d}(\delta x_{\mathrm{sl}}(t))}{\mathrm{d}t} = \delta(t) P_{x_{\mathrm{sl}}(t)}(D_x J(x)|_{x_{\mathrm{sl}}(\tau)})(\Delta(t)) \ ;$$

$$\delta x_{\mathrm{sl}}(t) = \int_0^t \delta(\tau) P_{x_{\mathrm{sl}}(\tau)}(D_x J(x)|_{x_{\mathrm{sl}}(\tau)})(\Delta(\tau)) \,\mathrm{d}\tau \ . \tag{15.11}$$

where $\delta(t)$ is the solution of (15.7).

(3) For a **static post-processing**, one uses stationary points of dynamic equations (15.3), or of their simplified versions (15.4),(15.7). Instead of (15.3) one gets:

$$D_x J(x)|_{x_{\mathrm{sl}}(t)} \delta x = -\Delta_{x_{\mathrm{sl}}(t)} \tag{15.12}$$

with the additional condition $P_{x_{\mathrm{sl}}} \delta x = 0$. This is exactly the iteration equation of the Newton method for solving the invariance equation. A clarification is in order here. Static post-processing (15.12) as well as other post-processing formulas should not be confused with the Newton method and others for correcting the approximately invariant manifold. Here, only the single trajectory $x_{\mathrm{sl}}(t)$ on the manifold is corrected, not the whole manifold.

The corresponding stationary problems for the model equations and for the projections of (15.3) on Δ are obvious. We only mention that in the projection on Δ one gets a step of the relaxation method for the invariant manifold construction.

In the following Example it will be demonstrated how one can use function $\Delta(x_{\mathrm{sl}}(t))$ in the accuracy estimation of macroscopic equations in the dynamics of polymer solution.

15.2 Example: Defect of Invariance Estimation and Switching from the Microscopic Simulations to Macroscopic Equations

A method which recognizes the onset and breakdown of the macroscopic description in microscopic simulations was developed in [29, 268, 414]. The method is based on the invariance of the macroscopic dynamics relative to the microscopic dynamics, and it is demonstrated for a model of dilute polymeric solutions where it decides switching between Direct Brownian Dynamics simulations and integration of constitutive equations.

15.2.1 Invariance Principle and Micro-Macro Computations

Derivation of reduced (macroscopic) dynamics from the microscopic dynamics is the dominant theme of non-equilibrium statistical mechanics. At the present time, this very old theme demonstrates new facets in view of a massive use of simulation techniques on various levels of description. A two-side benefit of this use is expected: On the one hand, simulations provide data on molecular systems which can be used to test various theoretical constructions about the transition from micro to macro description. On the other hand, while the microscopic simulations in many cases are based on limit theorems [such as, for example, the central limit theorem underlying the Direct Brownian Dynamics simulations (BD)] they are extremely time-consuming in any real situation, and a timely recognition of the onset of a macroscopic description may considerably reduce computational efforts.

In this subsection, we aim at developing a 'device' which is able to recognize the onset and the breakdown of a macroscopic description in the course of microscopic computations.

Let us first present the main ideas of the construction in an abstract setting. We assume that the microscopic description is set up in terms of microscopic variables ξ. In the examples considered below, microscopic variables are distribution functions over the configuration space of polymers. The microscopic dynamics of variables ξ is given by the microscopic time derivative $d\xi/dt = \dot{\xi}(\xi)$. We also assume that the set of macroscopic variables $\boldsymbol{M}$ is chosen. Typically, the macroscopic variables are some lower-order moments if the microscopic variables are distribution functions. The reduced (macroscopic) description assumes (a) The dependence $\xi(\boldsymbol{M})$, and (b) The macroscopic dynamics $d\boldsymbol{M}/dt = \dot{\boldsymbol{M}}(\boldsymbol{M})$. We do not discuss here in any detail the way one gets the dependence $\xi(\boldsymbol{M})$, however, we should remark that, typically, it is based on some (explicit or implicit) idea about decomposition of motions into slow and fast, with M as slow variables. With this, such tools as maximum entropy principle, quasi-stationarity, cumulant expansion etc. become available for constructing the dependence $\xi(\boldsymbol{M})$.

Let us compare the microscopic time derivative of the function $\xi(\boldsymbol{M})$ with its macroscopic time derivative due to the macroscopic dynamics:

$$\Delta(\boldsymbol{M}) = \frac{\partial \xi(\boldsymbol{M})}{\partial \boldsymbol{M}} \cdot \dot{\boldsymbol{M}}(\boldsymbol{M}) - \dot{\xi}(\xi(\boldsymbol{M})) \, . \tag{15.13}$$

If the *defect of invariance* $\Delta(\boldsymbol{M})$ (15.13) is equal to zero on the set of admissible values of the macroscopic variables M, it is said that the reduced description $\xi(\boldsymbol{M})$ is invariant. Then the function $\xi(\boldsymbol{M})$ represents the invariant manifold in the space of microscopic variables. The invariant manifold is relevant if it is stable. Exact invariant manifolds are known in a very few cases (for example, the exact hydrodynamic description in the kinetic Lorentz gas model [202], in Grad's systems [40, 42], and one more example will be mentioned below). Corrections to the approximate reduced description through minimization of the defect of invariance is a part of the so-called method of invariant manifolds [11]. We here consider a different application of the invariance principle for the purpose mentioned above.

The time dependence of the macroscopic variables can be obtained in two different ways: First, if the solution of the microscopic dynamics at time t with initial data at t_0 is ξ_{t,t_0}, then evaluation of the macroscopic variables on this solution gives $\boldsymbol{M}_{t,t_0}^{\mathrm{micro}}$. On the other hand, solving dynamic equations of the reduced description with initial data at t_0 gives $\boldsymbol{M}_{t,t_0}^{\mathrm{macro}}$. Let $\|\Delta\|$ be a value of defect of invariance with respect to some norm, and $\epsilon > 0$ is a fixed tolerance level. Then, if at the time t the following inequality is valid,

$$\|\Delta(\boldsymbol{M}_{t,t_0}^{\mathrm{micro}})\| < \epsilon \, , \tag{15.14}$$

this indicates that the accuracy provided by the reduced description is not worse than the true microscopic dynamics (the macroscopic description *sets on*). On the other hand, if

$$\|\Delta(\boldsymbol{M}_{t,t_0}^{\mathrm{macro}})\| > \epsilon \, , \tag{15.15}$$

then the accuracy of the reduced description is insufficient (the reduced description *breaks down*), and we must use the microscopic dynamics.

Thus, evaluating the defect of invariance (15.13) on the current solution to macroscopic equations, and checking the inequality (15.15), we are able to answer the question whether we can trust the solution without looking at the microscopic solution. If the tolerance level is not exceeded then we can safely integrate the macroscopic equation. We now proceed to a specific example of this approach. We consider a well-known class of microscopic models of dilute polymeric solutions

15.2.2 Application to Dynamics of Dilute Polymer Solution

A well-known problem of the non-Newtonian fluids is the problem of establishing constitutive equations on the basis of microscopic kinetic equations. We here consider a model introduced by Lielens et al. [410]:

$$\dot{f}(q,t) = -\partial_q \left\{ \kappa(t) q f - \frac{1}{2} f \partial_q U(q^2) \right\} + \frac{1}{2} \partial_q^2 f \; . \qquad (15.16)$$

With the potential $U(x) = -(b/2) \ln(1 - x/b)$ equation (15.16) becomes the one-dimensional version of the FENE dumbbell model which is used to describe the elongational behavior of dilute polymer solutions.

The reduced description seeks a closed time evolution equation for the stress $\tau = \langle q \partial_q U(q^2) \rangle - 1$. Due to its non-polynomial character, the stress τ for the FENE potential depends on all moments of f. We have shown in [411] how such potentials can be approximated systematically by a set of polynomial potentials $U_n(x) = \sum_{j=1}^{n} \frac{1}{2j} c_j x^j$ of degree n with coefficients c_j depending on the even moments $M_j = \langle q^{2j} \rangle$ of f up to order n, with $n = 1, 2, \ldots$, formally converging to the original potential as n tends to infinity. In this approximation, the stress τ becomes a function of the first n even moments of f, $\tau(\boldsymbol{M}) = \sum_{j=1}^{n} c_j M_j - 1$, where the set of macroscopic variables is denoted by $\boldsymbol{M} = \{M_1, \ldots, M_n\}$.

The first two potentials approximating the FENE potential are:

$$U_1(q^2) = U'(M_1) q^2 \qquad (15.17)$$

$$U_2(q^2) = \frac{1}{2}(q^4 - 2M_1 q^2) U''(M_1) + \frac{1}{2}(M_2 - M_1^2) q^2 U'''(M_1) \, , \; (15.18)$$

where U', U'' and U''' denote the first, second and third derivative of the potential U, respectively. The potential U_1 corresponds to the well-known FENE–P model. The kinetic equation (15.16) with the potential U_2 (15.18) will be termed the FENE–P+1 model below. Direct Brownian Dynamics simulation (BD) of the kinetic equation (15.16) with the potential U_2 for the flow situations studied in [410] demonstrates that it is a reasonable approximation to the true FENE dynamics whereas the corresponding moment chain is of a simpler structure. In [29] this was shown for a periodic flow, while Fig. 15.1 shows results for the flow

$$\kappa(t) = \begin{cases} 100t(1-t)e^{-4t} & 0 \le t \le 1 \; ; \\ 0 & \text{else} \, . \end{cases} \qquad (15.19)$$

The quality of the approximation indeed increases with the order of the polynomial.

For any potential U_n, the invariance equation can be studied directly in terms of the full set of the moments, which is equivalent to studying the distribution functions. The kinetic equation (15.16) can be rewritten equivalently in terms of moment equations,

$$\dot{M}_k = F_k(M_1, \ldots, M_{k+n-1}) \; ; \qquad (15.20)$$

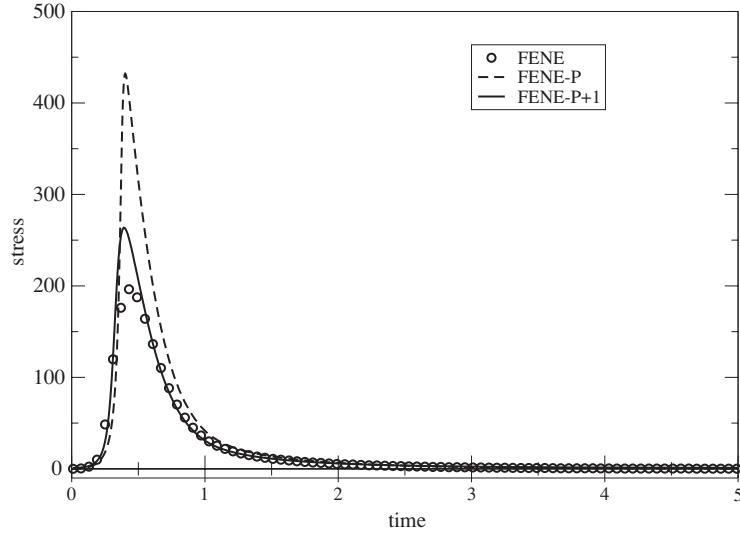$$F_k = 2k\kappa(t) M_k + k(2k-1) M_{k-1} - k \sum_{j=1}^{n} c_j M_{k+j-1} \; .$$

Fig. 15.1. Stress τ versus time from direct Brownian dynamics simulation: symbols – FENE, *dashed* line – FENE–P, *solid* line – FENE–P+1

We seek functions $M_k^{\mathrm{macro}}(\boldsymbol{M})$, $k = n+1, \ldots$ which are form-invariant under the dynamics:

$$\sum_{j=1}^{n} \frac{\partial M_k^{\mathrm{macro}}(\boldsymbol{M})}{\partial M_j} F_j(\boldsymbol{M}) = F_k(M_1, \ldots, M_n, M_{n+1}(\boldsymbol{M}), \ldots, M_{n+k}(\boldsymbol{M})) .$$

$$(15.21)$$

This set of invariance equations states the following: The time derivative of the form $M_k^{\mathrm{macro}}(\boldsymbol{M})$ when computed due to the closed equation for $\boldsymbol{M}$ (the first contribution on the left hand side of (15.21), or the 'macroscopic' time derivative) equals the time derivative of M_k as computed by true moment equation with the same form $M_k(\boldsymbol{M})$ (the second contribution, or the 'microscopic' time derivative), and this equality should hold whatsoever values of the moments $\boldsymbol{M}$ are.

Equations (15.21) in case $n = 1$ (FENE–P) are solvable exactly with the result

$$M_k^{\mathrm{macro}} = a_k M_1^k , \qquad \text{with} \quad a_k = (2k-1)a_{k-1}, \ a_0 = 1 .$$

This dependence corresponds to the Gaussian solution in terms of the distribution functions. As expected, the invariance principle give just the same result as the usual method of solving the FENE–P model.

Let us briefly discuss the potential U_2, considering a simple closure approximation

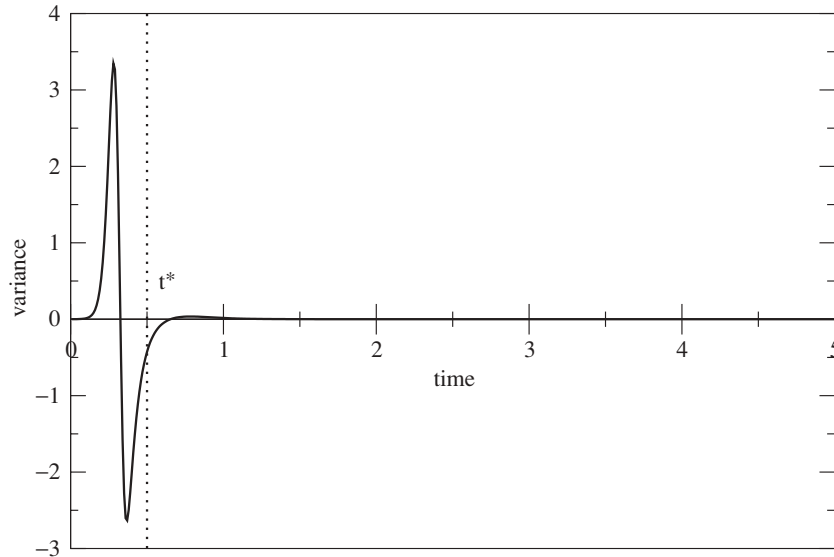$$M_k^{\mathrm{macro}}(M_1, M_2) = a_k M_1^k + b_k M_2 M_1^{k-2} , \tag{15.22}$$

Fig. 15.2. Defect of invariance Δ_3/b^3, (15.23), versus time extracted from BD simulation (the FENE–P+1 model) for the flow situation of (15.19)

where $a_k = 1 - k(k-1)/2$ and $b_k = k(k-1)/2$. The function M_3^{macro} closes the moment equations for the two independent moments M_1 and M_2. Note, that M_3^{macro} differs from the corresponding moment M_3 of the actual distribution function by the neglect of the 6-th cumulant. The defect of invariance of this approximation is a set of functions Δ_k where

$$\Delta_3(M_1, M_2) = \frac{\partial M_3^{\text{macro}}}{\partial M_1} F_1 + \frac{\partial M_3^{\text{macro}}}{\partial M_2} F_2 - F_3 \,, \qquad (15.23)$$

and analogously for $k \geq 3$. In the sequel, we make all conclusions based on the defect of invariance Δ_3 (15.23).

It is instructive to plot the defect of invariance Δ_3 versus time, assuming the functions M_1 and M_2 are extracted from the BD simulation (see Fig. 15.2). We observe that the defect of invariance is a nonmonotonic function of the time, and that there are three pronounced domains: From $t_0 = 0$ to t_1 the defect of invariance is almost zero which means that the ansatz is reasonable. In the intermediate domain, the defect of invariance jumps to high values (so the quality of approximation is poor). However, after some time $t = t^*$, the defect of invariance again becomes negligible, and remains so for later times. Such behavior is typical of so-called "kinetic layer".

Instead of attempting to improve the closure, the invariance principle can be used directly to switch from the BD simulation to the solution of the macroscopic equation without loosing the accuracy to a given tolerance. Indeed, the defect of invariance is a function of M_1 and M_2, and it can be easily
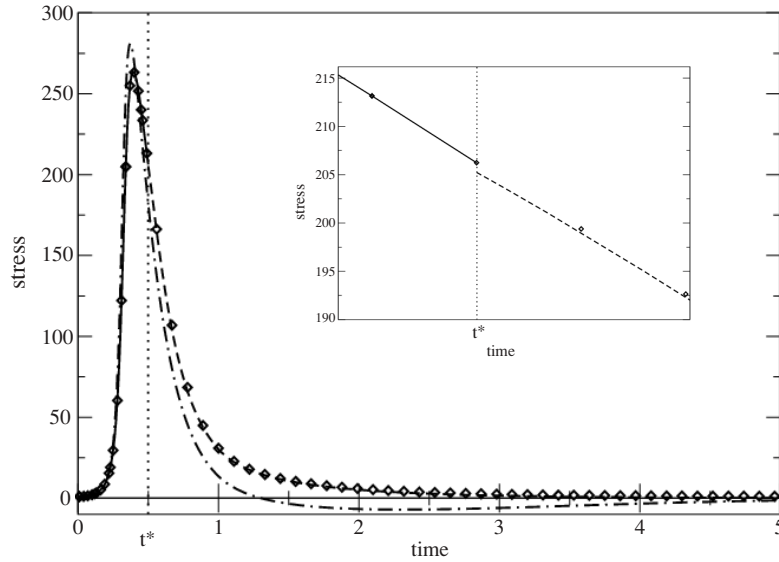
Fig. 15.3. Switching from the BD simulations to macroscopic equations after the defect of invariance has reached the given tolerance level (the FENE–P+1 model): symbols – the BD simulation, solid line – the BD simulation from time $t = 0$ up to time $t = t^*$, *dashed* line – integration of the macroscopic dynamics with initial data from BD simulation at time $t = t^*$. For comparison, the *dot-dashed* line gives the result for the integration of the macroscopic dynamics with equilibrium conditions from $t = 0$. Inset: Transient dynamics at the switching from BD to macroscopic dynamics on a finer time scale

evaluated both on the data from the solution to the macroscopic equation, and the BD data. If the defect of invariance *exceeds* some given tolerance on the macroscopic solution this signals to switch to the BD integration. On the other hand, if the defect of invariance becomes *less* than the tolerance level on the BD data signals that the BD simulation is not necessary anymore, and one can continue with the integration of the macroscopic equations. This reduces the necessity of using BD simulations only to get through the kinetic layers. A realization of this hybrid approach is demonstrated in Fig. 15.3: For the same flow we have used the BD dynamics only for the first period of the flow while integrated the macroscopic equations in all the later times. The quality of the result is comparable to the BD simulation whereas the total integration time is much shorter. The *transient dynamics* at the point of switching from the BD scheme to the integration of the macroscopic equations (shown in the inset in Fig. 15.3) deserves a special comment: The initial conditions at t^* are taken from the BD data. Therefore, we cannot expect that at the time t^* the solution is already on the invariant manifold, rather, at best, close to it. Transient dynamics therefore signals the *stability* of the

invariant manifold we expect: Even though the macroscopic solution starts
not on this manifold, it nevertheless attracts to it. The transient dynam-
ics becomes progressively less pronounced if the switching is done at later
times. The stability of the invariant manifold in case of the FENE–P model
is studied in detail in [109].

The present approach of combined microscopic and macroscopic simu-
lations can be realized on the level of moment closures (which then needs
reconstruction of the distribution function from the moments at the switch-
ing from macroscopic integration to BD procedures), or for parametric sets of
distribution functions if they are available [410]. It can be used for a rigorous
construction of domain decomposition methods in various kinetic problems.